WDS'14 Proceedings of Contributed Papers — Physics, 199–203, 2014. ISBN 978-80-7378-276-4 © MATFYZPRESS

Study of Alfven Eigenmodes in Tokamak COMPASS

T. Markovic, J. Stockel, and J. Seidl

Institute of Plasma Physics AS CR, v.v.i., Prague, Czech Republic.

A. Melnikov

Institute of Tokamak Physics, NRC 'Kurchatov Institute', Moscow, Russian Federation.

S. Medvedev

Keldysh Institute of Applied Mathematics, RAS, Moscow, Russian Federation.

Abstract. Having both MHD and kinetic character plasma Alfven eigenmodes are significant not only on the field basic plasma research, but also on the field of magnetic confinement fusion. An introduction to basic physical principles of Alfven eigenmodes under MHD approximation is provided. Presented results of recent experiments on COMPASS suggest occurrence of toroidal Alfven eigenmodes in this tokamak, which is further supported by preliminary linear MHD code simulations, althought more studies will have to be conducted in the future to further investigate presented modes therein.

Introduction

Alfven waves have been subject of interest to fusion community since 70's. At the time, the main topic of interest was plasma heating scheme via kinetic absorption of antenna-generated wave in continuum part of Alfven spectrum [*Chen and Hasegawa*, 1974], however this interest soon shifted towards study of Alfven spectrum gap modes. It was discovered both theoretically and experimentally that gap modes might interact with superalfvenic fusion products, and induce loss of their confinement before thermalization can take place. This effect would have negative impact on fusion yield and might lead to wall damage [*Wong*, 1998; *Heidbrink*, 2008; *Sharapov*, 2013]. This work provides insight into basic physical principles and spatial structure of Alfven continuum and gap modes, using magnetohydrodynamic (MHD) description (implying that kinetic effects and growth/damping mechanisms are not covered here. Interested reader is refered to [*Heidbrink*, 2008; *Pinches*, 1996; *Chen and Hasegawa*, 1974]). Paper also contains first preliminary results of study of Alfvenic gap modes in tokamak COMPASS, observed in spectra of perturbation of measured plasma quantities.

Basic Physics of Alfven Modes

Alfven Continuum

Taking ideal MHD equations into consideration and by request that maximum-order quantity perturbations to be linear, one can derive vector equation [*Sharapov*, 2013]:

$$\frac{\partial^2 \boldsymbol{\xi}}{\partial t^2} = c_s^2 \nabla(\nabla \cdot \boldsymbol{\xi}) + v_A^2 \nabla_\perp (\nabla \cdot \boldsymbol{\xi}_\perp) + v_A^2 \frac{\partial^2 \boldsymbol{\xi}_\perp}{\partial z^2}. \tag{1}$$

In above relation, quantity c_s represents ion sound speed (relation between plasma equilibrium pressure and density), $\mathbf{v_A} = \frac{\mathbf{B_0}}{\sqrt{\mu_0 \rho_0}}$ is Alfven velocity and finally, displacement vector $\boldsymbol{\xi}$ is defined via plasma linear velocity perturbation as $\mathbf{v_1} = \frac{\partial \boldsymbol{\xi}}{\partial t}$. Symbol $\perp$ refers to direction perpendicular to $\mathbf{B_0}$. There are three possible solutions of equation (1), of which the non-compressible branch — shear Alfven waves, is the one that is relevant for this study.

Shear Alfven waves propagate in direction parallel to $\mathbf{B_0}$ vector and are of transversal character. For homogeneous plasma, by putting harmonic-character perturbations of $q = q_0 \exp[\mathrm{i}(\mathbf{k} \cdot \mathbf{x} - \omega t)]$, it is straightforward to show that for non-compressible Alfven waves, equation (1) yields dispersion relation of

$$\omega^2 = (\mathbf{k} \cdot \mathbf{v_A})^2 = \text{const.} \tag{2}$$

Waves that comform to this relation are refered to as *Alfven continuum*. In standard experimental plasma, ρ_0 is a function of spatial coordinate, while wavevector $\mathbf{k}$ is subject to periodicity constraints,

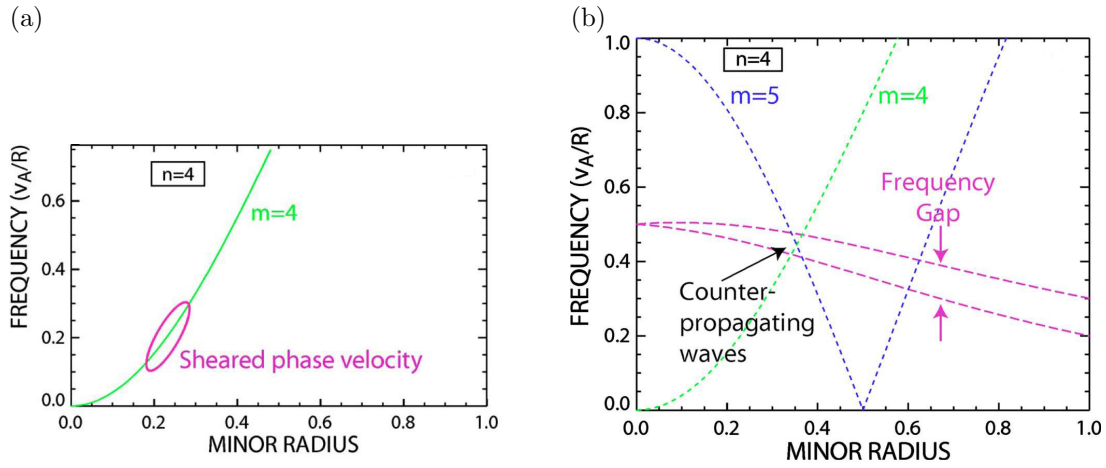

Figure 1. (a) Shear in phase velocity of Alfven continuum waves for given m and n structure, coming from equation (3) [*Heidbrink*, 2008]. (b) Frequency (phase velocity normalized to R) of counter-propagating shear Alfven waves of different poloidal structure, given by m. [*Heidbrink*, 2008].

given by geometry of the device. For helical field lines of toroidal tokamak plasma [*Heidbrink*, 2008]:

$$\omega^2(r) = (k_{\parallel}(r)v_A(r))^2 \quad \text{with} \quad v_A(r) = \frac{B_0}{\sqrt{\mu_0\rho_0(r)}} \quad \text{and} \quad k_{\parallel}(r) = \frac{1}{R}\left(n - \frac{m}{q(r)}\right). \tag{3}$$

Quantity R represents major radius of torus, r distance from plasma center, n and m stand for toroidal and poloidal number of mode periodicity respectively and q represents inverse of rotational transform of field line. As can be seen in Fig. 1a, plasma inhomogenity induces a strong shear in Alfven continuum, which is responsible for strong damping of continuum waves via mechanism of phase mixing — specifically with coefficient of: $\gamma \sim \frac{\partial k_{\parallel} v_A}{\partial r}$. The damping is of resonant character, being localized in a very narrow radial layer. Exact mechanism of damping is however beyond MHD approximation and interested reader should refer to review articles of [*Wong*, 1998; *Heidbrink*, 2008].

Toroidal Alfven Eigenmodes (TAE)

In toroidal plasmas, as Alfven wave propagates in parallel with helical fieldlines on given r, it encounters modulation of its phase velocity $v_A = \frac{B_0}{\sqrt{\mu_0\rho_0}}$. This is due to modulation of B_0 quantity, and althought there are several causes of this (plasma ellipticity, triangularity, etc.), the dominant effect comes from plasma toroidicity of $B_0 \sim \frac{1}{R}$ [*Sharapov*, 2013; *Heidbrink*, 2008]. The resultant periodicity in refraction index allows for reflection of wave. Additionally, due to dependency of $k_{\parallel}$ on n and m mode numbers (see eq. (3)), it is possible for two different, counterpropagating waves to share their frequency on given radius — see Fig. 1b). Resultant destructive interference of the two waves generates a Bragg gap of forbidden frequencies in Alfven continuum, centered around

$$f_B \approx \frac{1}{4\pi Rq}\frac{B_0}{\sqrt{\mu_0 m_i Z_{\text{eff}} n_e}}. \tag{4}$$

In above equation, m_i represents effective ion mass (assuming single-component plasma), Z_{eff} effective charge of ions and n_e electron density (which is less challenging to measure than ion density). The details of the whole coupling process are rather mathematically complex and interested reader is refered to [*D'Ippolito*, 1980] and [*Cheng, et al.*, 1985].

Nontrivially, albeit in analogy to solid state physics — propagation of electron wave in Briollin zones of crystal lattice (see [*D'Ippolito*, 1980] for further reference), a specific type of waves can exist within the Alfven continuum gap. These gap modes are refered to as toroidal Alfven eigenmodes (TAE), since the gap in itself was primarily induced by plasma toroidicity effects. As they do not belong to continuum part of spectrum, they are no longer subject to strong phase-mixing damping and have subsequently lower demands on driving mechanisms. Additionally, unlike Alfven continuum waves, they are tractable with MHD approximation, being represented as coupling and superposition of two waves of m and $m+1$ poloidal harmonics. There are two possible combinations of the m and $m+1$ harmonics for a given mode — either constructive interference in higher R area (low-field side or LFS, with reference to B_0

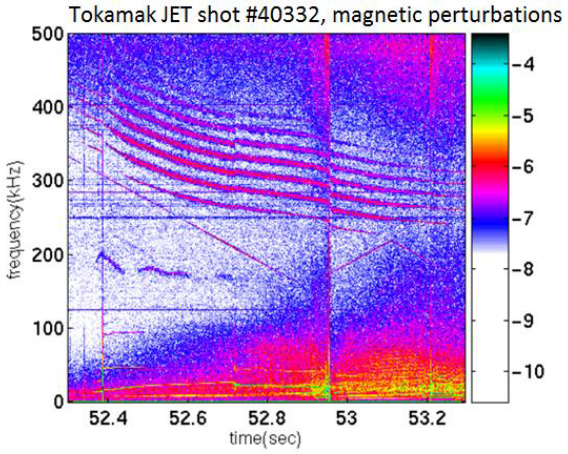

Figure 2. TAE observed in tokamak JET. Power spectrum of local fluctuations, detected by magnetic pick-up coils outside plasma [*Sharapov*, 2013].

magnitude) and destructive interference in lower R area (high-field side or HFS), or vice versa — see Fig. 4. The former case with lower frequency is refered to as *ballooning* mode, while latter, higher frequency mode, is being refered to as *anti-ballooning* mode.

It is common for more TAEs with different, but similar m and n structure to be present in plasma at the same time. In that case, their frequency in laboratory frame is Doppler shifted by toroidal plasma rotation f_{rot}, like any other MHD mode [*Turnbull, et al.*, 1993]:

$$f_{\mathrm{TAE}} \approx f_B + n \cdot f_{\mathrm{rot}}. \tag{5}$$

Additionally, it can be seen from equation (4), $f_B \sim \frac{1}{\sqrt{n_e}}$, and since quantity n_e changes over the discharge duration, so does frequency of eventual TAE modes. Combined effect of above-mentioned mechanisms can be seen in Fig. 2. On spectrogram, TAE modes are seen as very high-frequency bands, distanced from each other by plasma toroidal rotation frequency and their different structure. Gradual decrease of mode frequency corresponds to increase in n_e.

Alfven Mode Observations in Tokamak COMPASS

Experimental Methods

MHD modes in general are detected as local fluctuations of global plasma quantities, such as current distribution (perturbations of magnetic field B), plasma (or floating) potential φ, n_e etc. Heavy ion-beam probing of plasma seems thus optimal for study of MHD phenomena, since this diagnostics allows for simultaneous detection of n_e, ξ_r and φ [*Melnikov, et al.*, 2010]. However, in order to study Alfven eigenmode phenomena in tokamak COMPASS, more readily available MHD detection means were utilized — measurements of local B fluctuations across poloidal direction by array of magnetic pick-up coils, and measurements of fluctuations in potential by means of Langmuir and ball-pen probe on horizontal reciprocating manipulator. While former diagnostics provide specification of ballooning/anti-ballooning character, mode frequency evolution and m and n mode number estimates, the latter allow for radial localization of eventual balloning modes.

Besides processing the measured fluctuations into power spectrum, a more advanced method of normalized coherence (as in [*Melnikov, et al.*, 2012]) was used as well:

$$\mathrm{Coh}_{xy}(f,t) = \frac{|S_{xy}|}{\sqrt{|S_{xx}S_{xy}|}}. \tag{6}$$

Quantity S_{xx} is auto-power spectrum of quantity x, while S_{xy} stands for cross-power spectrum. The method essentially represents mean of spectral product, normalized to [0,1] interval. Among its advantages, it supresses non-coherent noise and allows for better monitoring of coherent modes. Its main drawback is worse temporal or frequency resolution than that of equivalent power spectrum.

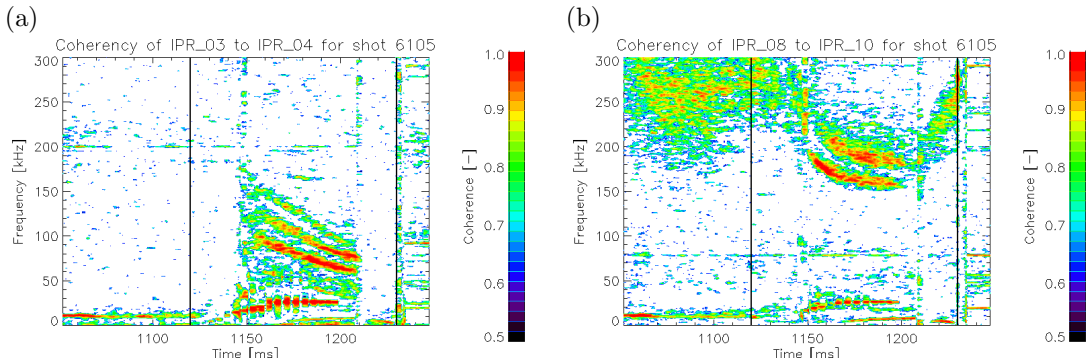

Figure 3. Normalized coherence of discharge 6105. Black vertical lines represent NBI switching on and off. (a) Coils on LFS showing ballooning modes. (b) Coils on HFS showing anti-ballooning modes.

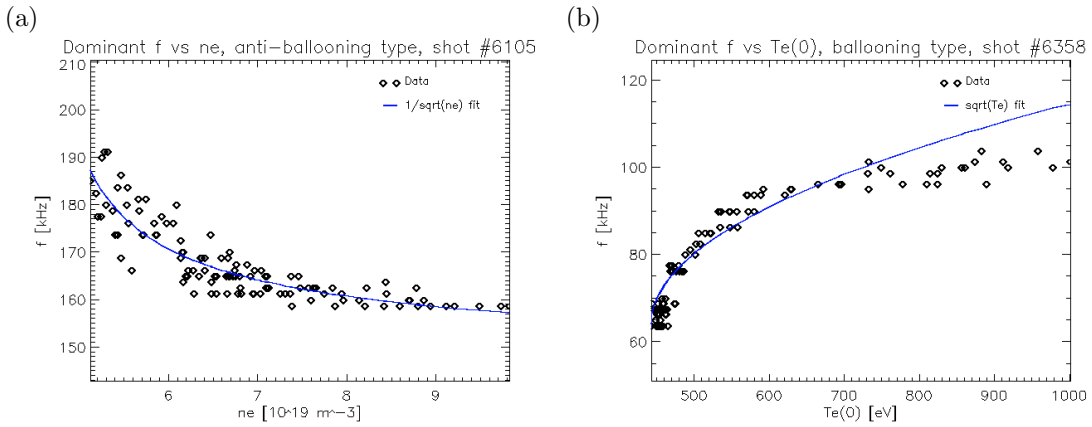

Figure 4. (a) Scaling of one of anti-ballooning modes with n_e, with $\frac{1}{\sqrt{n_e}}$ fit curve. (b) Scaling of one of ballooning modes with T_e, with $\sqrt{T_e}$ fit curve.

Observations and Discussion

Coherency plots in Fig. 3 show the main candidates for TAE modes in tokamak COMPASS. These modes are characteristic for high-density, advanced plasma confinement modes (so called H-modes), over phases without presence of edge-localized modes (or ELMs). This high-density criterion is equivalent to requirement of $v_A < v_{\text{crit}}$ and might give implications of possible mode drive for future studies, since it appears that modes are not exclusively driven by externally injected high energetic particles (NBIs). The modes also appear to rotate in electron diamagnetic drift direction, which is unlikely, but not impossible for TAE modes. On the other hand, both ballooning and anti-ballooning modes are present paralelly, with anti-ballooning modes being of higher frequency than ballooning ones — as it woud be expected from TAEs.

Fig. 4a further shows frequency $\sim \frac{1}{\sqrt{n_e}}$ scaling of a sample anti-ballooning mode, which further supports the hypothesis, that it indeed might be TAE. On the other hand, $\sim \sqrt{T_e}$ scaling of ballooning mode sample in Fig. 4b would imply compressible Alfven wave character of these modes. It should be noted, that shown scalings represent only specific type of modes — in fact, anti-ballooning modes were not found to be scaled with $\sim \sqrt{T_e}$ and ballooning modes did not always scale with $\sim \frac{1}{\sqrt{n_e}}$.

Modes are also prevalent in spectra of potential fluctuations, measured by Langmuir and ball-pen probes in divertor region. Coherency of magnetic pick-up coils with probes installed on horizontal reciprocating manipulator imply, that observed ballooning modes are located close to separatrix (plasma edge). Anti-balooning modes can not be reached with this manipulator and thus experiments utilizing vertical reciprocation from the top of vessel will be necessary.

An addition to experimental observations, linear MHD code KINX [*Villard, et al.*, 1997] with respective COMPASS equilibria as an input, was utilized in order to provide approximate calculations of expected TAE characteristics. Besides reconstruction of spatial distribution of ballooning and anti-ballooning structure (see Figs. 5a and 5b), including m and n number, it also provided reconstruction

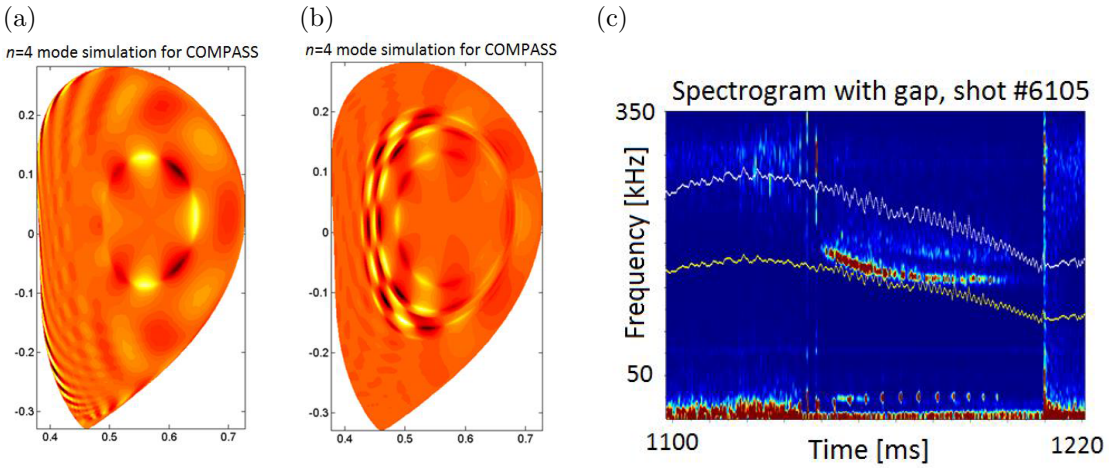

Figure 5. Results of preliminary KINX modeling of COMPASS plasma. (a) Ballooning mode structure for discharge 6105. (b) Anti-ballooning mode structure for discharge 6105. (c) Evolution of Bragg gap over HFS coil spectrogram.

of Alfven continuum gaps (see Fig. 5c). The preliminary calculation identified anti-ballooning mode to lie within respective Bragg gap, which would further support the statement that anti-ballooning modes are TAE, while ballooning modes might be of comressible wave character.

Conclusion

Each of the MHD Alfven modes, either from continuum of gap part of Alfven spectrum, has a specific signature of m and n mode number. While continuum modes consist of single m harmonic, TAE modes are due to their character a superposition of m and $m+1$ harmonic, which can be either of ballooning or anti-ballooning charater, whose frequency is slightly higher that that of former case. Several such modes standardly appears in parallel and their rotation slows down, as n_e increases. All of this was observed in low v_A, high-confinement plasmas of tokamak COMPASS. Moreover, preliminary calculations with KINX code also imply that, at least anti-ballooning modes, might be TAE. Neveretheless, more experiments are necessary, in order to disclose the actual driving mechanism of these modes and to do dedicated comparison of mode m and n structure to those from the model.

Acknowledgments. This project was partly supported by MSMT Project no. LM2011021.

References

Chen, L., and A. Hasegawa, Plasma heating by spatial resonance of Alfven wave, *The Physics of Fluids*, 17, 1399–1403, 1974.

Cheng, C. Z., L. Chen and M. S. Chance, High-n Ideal and Resstive Shear Alfven Waves in Tokamaks, *Annals of Physics*, 161, 21–47, 1985.

D'Ippolito, D. A., and J. P. Goedbloed, Mode coupling in a toroidal sharp-boundary plasma — I. Weak-coupling limit, *Plasma Physics*, 22, 1091–1107, 1980.

Heidbrink, W. W., Basic physics of Alfven instabilities driven by energetic particles in toroidally confined plasmas, *Physics of Plasmas*, 15, 055501, 2008.

Melnikov, A. V., et al., Internal measurements of Alfven eigenmodes with heavy ion beam probing in toroidal plasmas, *Nucl. Fusion*, 50, 084023, 2010.

Melnikov, A. V., et al., Alfven eigenmode properties and dynamics in the TJ-II stellarator, *Nucl. Fusion*, 52, 123004, 2012.

Pinches, S.D., Nonlinear interaction of fast particles with Alfven waves in tokamaks, Doctoral Dissertation, University of Nottingham, 1996.

Sharapov, S. E., Fast ions and MHD waves, *Proceedings of 11th Carolus Magnus Summer School*, Bad Honnef, 2013.

Turnbull, A. D., et al, Global Alfven modes: Theory and experiment, *Phys. Fluids B*, 5, 2546–2553, 1993

Villard, L., et al, The KINX indeal MHD stability code for axisymmetric plasmas with separatrix, *Computer Physics Communications*, 103, 10–27, 1997

Wong, K.-L., A review of Alfven eigenmode observations in toroidal plasmas, *Plasma Phys. Control. Fusion*, 41, R1–R56, 1999.